IEEE International Electric Machines & Drives Conference

Miami, FL - May 21-24, 2017

Conference Program

IEEE PES Power & Energy Society®

pels IEEE POWER ELECTRONICS SOCIETY Powering a Sustainable Future

IAS IEEE INDUSTRY APPLICATIONS SOCIETY Linking Research to Practice

ICS

ENERGY SYSTEMS RESEARCH LABORATORY

Multiphysical Design Methodology of a High-Speed Induction Motor for a Kinematic-Electric Powertrain

Daniel Butterweck[1], Marco Hombitzer[1], Kay Hameyer[1]
[1]Institute of Electrical Machines (IEM), RWTH Aachen University, 52062 Aachen, Germany

***Abstract*—This paper describes a multiphysical methodology developed to design a high-speed induction motor for a technically complicated kinematic-electric powertrain. The main focus lies on the definition of realistic load cycles and the possibility to rapidly refine the motor design and the operating strategy of the powertrain based on results from thermal, structural and vehicle simulations.**

Keywords— Electrical Machines, Design, Induction Machine, High-Speed Drive

I. Introduction

For an efficient design and operation of electrical machines, the definition of representative load cycles and requirement specifications are crucial. These are largely dependent on the distribution of the drives operating points. Specifications of drives designed for industrial applications are usually well defined by a small number of operating points. In case of the design of traction drives for automotive applications, the motor is operated in multiple operating points. For simple drivetrain topologies with only one electric motor as in electric vehicles (EV), the operating points are directly linked to the vehicle speed and can be prescribed by a driving cycle. In case of more complicated drivetrains consisting of several machines, the operating points of the motor strongly depend on the operating strategy. In both cases, the operating strategy of the drivetrain is usually considered fixed during the motor design process [1, 2 and 3]. By employing a combined development of the electric machine and the operating strategy, additional degrees of freedom for the motor designer arise, and a satisfying performance of the entire drivetrain can be achieved. Therefore, the possibility to generate realistic load cycles for all components involved, taking the operating strategy into account, is required. On the other side, a rapid feedback of the current motor designs performance in regards of thermal and structural dynamic problems, as well as its overall efficiency in context of the whole powertrain is required for the refinement of the motor design and its operating strategy. In this paper, such a methodology is developed for the design of a high-speed induction motor used in a complicated kinematic-electric powertrain. The methodology combines electromagnetic finite element analysis (FEA), a vehicle model including the powertrain and its operating strategy, transient thermal simulations of the motor and structural FEA of the high-speed rotor.

II. Kinematic-Electric-Powertrain

In the research project "KinelectricDrive", a kinematic-electric powertrain for small vehicles is developed and prototypically built up. Figure 1 shows the schematic of the powertrain developed. Central component of the system is the flywheel motor consisting of a 48 Volt high-speed induction motor (IM) and a highly integrated flywheel (FW) with a speed up to 45,000 rpm. To reduce drag losses, the induction machine and the flywheel are operated under a rough technical vacuum up to 7 mbar. Additionally, an electric infinite variable transmission (eIVT) is employed to decouple the flywheel speed from the powertrain output speed. The eIVT consists of a planetary gear set where the ring gear is powered by a permanent magnet electric motor. By controlling the speed of the ring gear, the output speed of the drive system can be adjusted to match the drivers' request independent of the flywheel speed and its kinetic energy stored. Equation (1) describes the dependencies of the three speeds. The speeds are linked by the gear train ratio $i_0 = -5$.

$$n_{Flywheel} + (i_0 - 1)\, n_{Output} - i_0\, n_{Ring} = 0 \qquad (1)$$

The powertrain described allows to buffer energy gained by recuperation in the kinetic power path and to use it at later times to accelerate the vehicle. With this strategy, high power peaks in the electric path can be avoided. The battery is therefore less strained and its lifetime increases. In addition, a higher mechanical output power than in full electric 48 Volt drivetrains can be achieved when the high speed induction motor is operated in generator mode [4]. The Systems targeted field of applications are the hybridization of gears and all-wheel drives, main traction drive of small electric vehicles aswell as start/stop generator with boost- and recuperation functions.

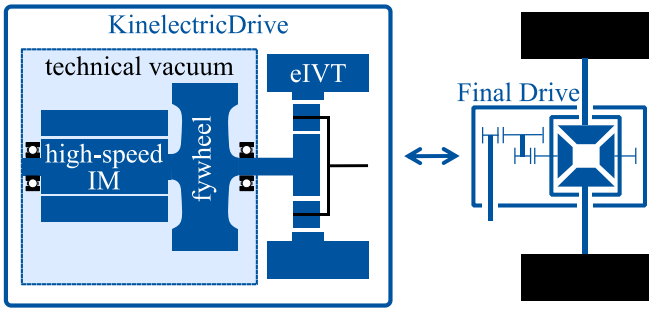

Fig. 1: Schematic overview of the powertrain developed.

This paper was developed in the context of the cooperative project 'KinelectricDrive', sponsored by the German Federal Ministry of Economic Affairs and Energy (BMWi), reference number 01MY14006B.

978-1-5090-4281-4/17/$31.00 ©2017 IEEE

III. Desing Methodology

The design methodology followed for the high-speed IM consists of mainly five steps. Figure 2 shows the general relations of the design steps. Based on the constraints and requirement specifications (e.g. desired performance data, available installation space and target costs) of the desired application, an initial design is outlined with the aid of an analytical motor model following the standard design criteria. After an appropriate design is found, electromagnetic finite element analysis (EM-FEA) are carried out to calculate the motor's efficiency and loss maps. These maps are embedded in a vehicle model. The vehicle model is used to develop and refine the operating strategy of the powertrain based on driving performance and energy management as well as evaluating the interaction of the eIVT and the flywheel motor. For the subsequent design steps, load cycles for all components are derived by the vehicle model. These load cycles are used for the transient thermal simulations of the motor. Based on the simulated temperature profiles, refinements of the operating strategy are performed. In addition, the influence of e.g. the cooling system and the interfaces between the components like the fit between the stator outer face and the housing, can be examined. Once a thermally permissible operation of the motor is achieved, critical operation points in regard to mechanical firmness are identified and structural FEA of the rotor assembly are carried out. If necessary, a refinement of the design or the operating strategy is done. If a major impact of the design refinement on the motor's efficiency or loss distribution is expected, the motor maps will be recalculated. The design steps mentioned will be described in more detail in the following sections.

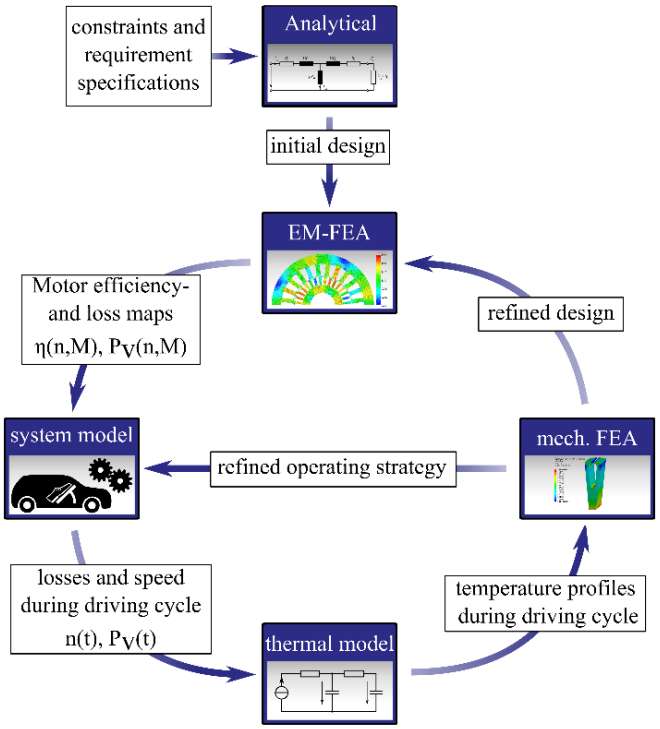

Fig. 2: Design methodology followed.

A. Analytical Model

Based on guideline values for flux- and current densities, the magnetic circuit and the stator winding are dimensioned following the standard design criteria [5]. For the field of application outlined, only drive topologies with low no-load losses are applicable in respect of a low self-discharge of the flywheel. Therefore permanent magnet motors, although they achieve a higher power density and lower rotor temperatures, are less appropriate. An induction motor is used to control the flywheel. To achieve the required power density and to reduce the rotor winding losses a copper squirrel cage rotor is used. Since the iron losses are largely influenced by the fundamental frequency of the stator current, the number of poles should be kept small in case of high-speed drives. Consequently, a 4-pole distributed 3-phase winding with 24 stator slots is applied, resulting in a maximum fundamental frequency of 1500 Hz. The pole pairs are connected in parallel to reduce the current inside the stator slot by half and to achieve the desired corner speed of 18,000 rpm. This results in a total number of two windings per slot. Due to skin-effects occurring at maximum fundamental frequency and manufacturing costs, hair pin windings are not considered for the prototypical build up motor. Instead, a wire-wound coil winding consisting of 15 parallel AWG 17 subconductors is applied. The peak current is limited to 400 Ampere, leading to an electric peak power of approximately 19 kW. This results in a peak current density of 12.81 A/mm^2 per subconductor. In case of inverter-fed induction motors, having a higher number of rotor slots than stator slots increases the overload capability of the motor. However, skewing should be avoided with regard to additional losses due to cross currents occurring between the rotor bars if skewed. Due to the damping effect of the flywheel, torque ripples are expected to have a minor impact. For this application, an unskewed rotor with 32 rotor bars is considered in regards of a low acoustic profile, circumferential speed and available installation space. The Motor finally has a stack length of 55.2 mm and 125 mm stator outer diameter. For the operation in a technical vacuum, a mica based insulation material is used to avoid the partial discharges and consequently a breakdown of the winding. The cross-section of the motor with 32 rotor slots is shown in Figure 3.

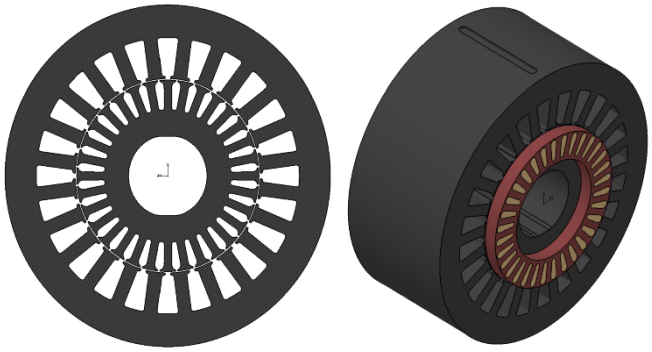

Fig. 3: Cross-section of the high-speed induction motor with 24 stator slots and 32 rotor slots (left) and isometric view with rotor squirrel cage (right).

B. *Electromagnetic FEA*

For the evaluation and refinement of the motor design, an accurate representation of the drive is required for the entire operation range. In contrast to analytical calculations based on the motors equivalent circuit as in [6], EM-FEA allow the more accurate representation of different loss mechanisms and measured soft magnetic material properties at the cost of a-priori computation time. It is therefore suitable to simulate the motor for the entire operating range and calculate the efficiency and loss maps as a function of torque and speed. In the present case, a total of 175 2D-FE simulations, with variations of stator phase current ranging from 0 Ampere to 400 Ampere and rotor slip frequency ranging from 0 % to 3 %, are performed on a computer cluster. In post-processing, the local iron loss distributions are calculated taking higher harmonics into account [7]. Several grades of low loss electrical steels are evaluated. For the present application, the electrical steel of the rotor must provide a high mechanical strength. In respect of a high motor efficiency low iron losses should be achieved especially in the stator of the motor. The electrical steel ultimately used for the stator and rotor core is Thyssen Krupp Steel Europe's 280-30AP, providing a good trade-off between low iron losses and mechanical strength. Using the same electrical steel for the rotor and the stator core additionally allows an economical manufacturing. Figure 3 shows the simulated efficiency map and the map of total losses of the motor. A good efficiency over the whole operating region is achieved. In the described design methodology, maps of the stator- and rotor iron- and copper losses as a function of torque and speed are incorporated into the system model, respectively.

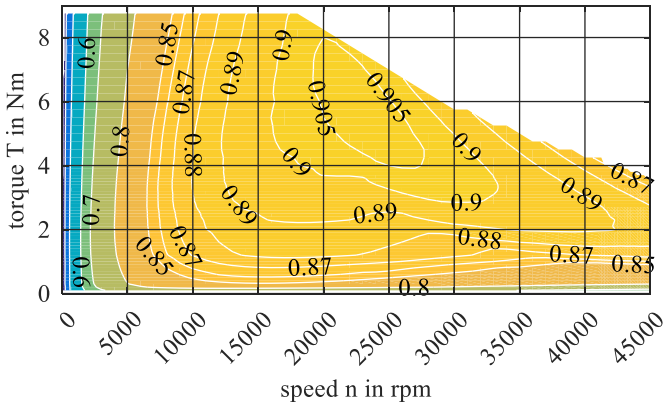

Fig. 4: FE-simulated efficiency map of the IM with 32 rotor slots.

C. *System model*

To evaluate the designs performance in the overall context of the drivetrain, a vehicle model is developed in MATLAB/Simulink. Due to the nature of the system, the operating points of the motor are non-deterministic and strongly depend on the operating strategy of the flywheel motor. Therefore, the model is also used to develop and refine the operating strategy in regards to the vehicle performance, energy management and battery charge. Ultimately, duty cycles for the design are derived. A schematic representation of the model is shown in figure 5.

The targeted vehicle speed is defined by a driving cycle. A driver is modeled by a PID-controller which results in a desired torque at the wheels of the vehicle. The final drive gear is modeled with a fixed gear ratio and the gear efficiency map as function of speed and torque in drive and coast mode. This defines the desired output torque of the kinelectric drive system. With the aid of the planetary gear equation set, the desired torque at the flywheel and the ring gear motor are calculated. Based on the current operating point and possible limitations of the drives, the actual torque of the motors and therefore the actual output torque are calculated. The actual vehicle speed is then calculated by the vehicle model which is described by a longitudinal model calculating the driving resistances taking drag, rolling friction and slopes into account. By controlling the induction motor, the power pathing inside the system is managed. From the motor speed, the torque provided and the efficiency at the current

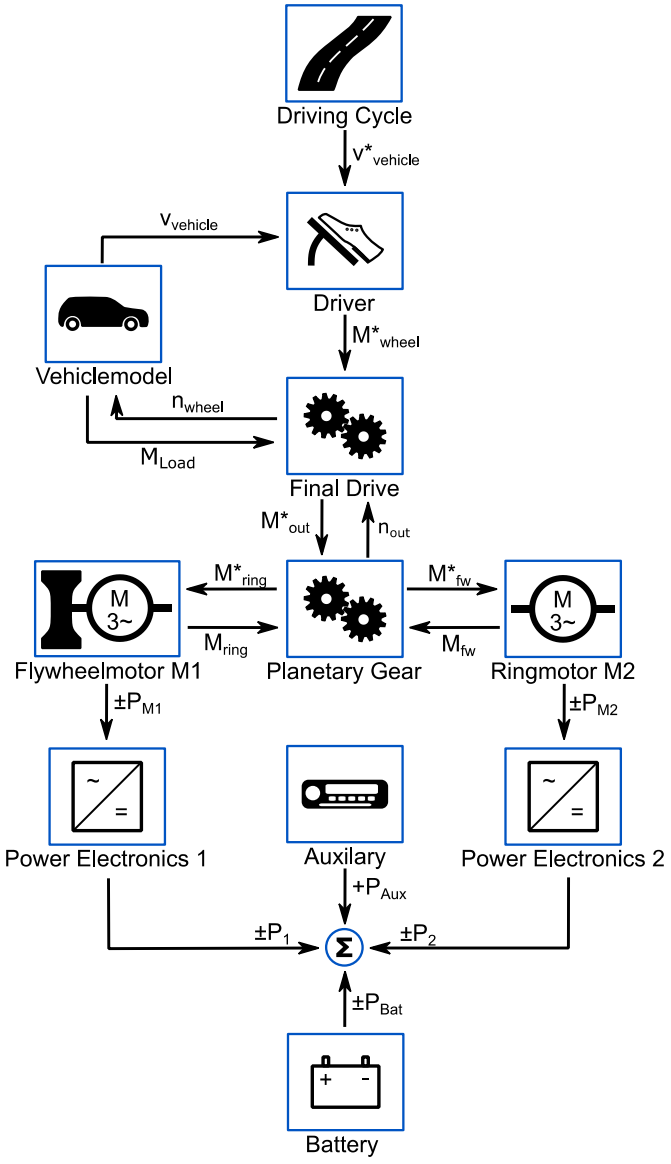

Fig. 5: Schematic overview of the kinelectric drive vehicle model.

operating point, the desired electrical power of the motor is calculated. The power electronics are described by an efficiency map allowing to calculate the requested electrical power of the high-speed path. Additionally taking the requested electrical power of the eIVT and possible auxiliary loads into account, a power balance can be calculated. The resulting electric energy has to be provided by or stored into the battery respectively. For the design of the motor, a WLTP class 3 driving cycle is simulated to derive the operating points of the motor during the driving cycle. By this method, time dependent loss profiles of the motor are gained. These loss profiles are shown in figure 6.

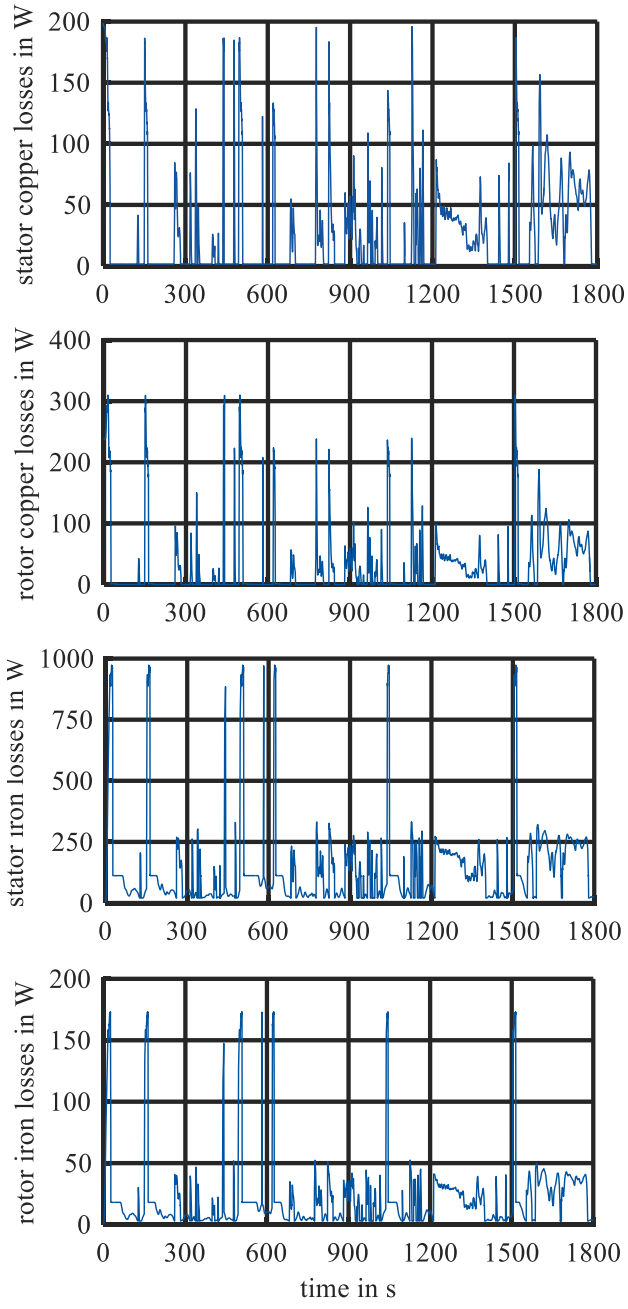

Fig. 6: Loss profiles for the high speed IM during one run of WLTP driving cycle.

D. Thermal model

The thermal simulation of the motor is of particular importance to ensure a safe and highly utilized operation. Especially for traction drives with several operating points, the determination of a continuous output power is of secondary interest. Therefore, transient simulations are necessary to give a good indication of the temperatures during specific load cycles. However, the quality of the results are strongly influenced by the cooling system, the materials used as well as manufacturing issues such as impregnations goodness and interfaces between components. With the aid of the commercial software Motor-CAD, a lumped parameter thermal model is generated based on the motor geometry. In contrast to FEM thermal simulations, the lumped parameter models allow a fast computation of complete load cycles. The software includes algorithms to model complex thermal phenomena dealing with the aforementioned features [8]. Since Motor-CAD only allows the use of pre-defined geometries, simplifications are done. Therefore, only the vacuum chamber, including the high-speed induction motor, is modeled in the geometry section. The flywheel is added as an additional thermal capacitance on the motor shaft in the thermal network. The eIVT is modeled by a fixed temperature of 80 °C at the mounting plate, given by the maximum temperature of the transmission oil. The cooling of the motor is achieved by a stator water jacket. As cooling fluid, water with 70 °C and 8 l/min is used. To reduce the drag losses, the flywheel motor is operated under a rough vacuum which causes reduced convective heat transfer. The vacuum is modeled by a flooded cooling option inside the housing with the fluid properties of air at 7 mbar. The fluid is described by its thermal conductivity, density, thermal capacitance as well as the kinematic viscosity. As described in [9], the thermal conductivity above 1 mbar can be assumed equal to that at atmospheric pressure. The density at 7 mbar is calculated by the ideal gas law. For the transient thermal simulation, the duty cycle is defined by the losses during three consecutive runs of a WLTP driving cycle simulated by the system model. At the third run, the system reached a temperature equilibrium. The resulting temperature profile of the third run is shown in Figure 4. At the start of the duty cycle, the vehicle is at standstill and the flywheel is accelerated from 0 rpm to 45,000 rpm by the induction motor (Point A in figure 7). In this case, the highest temperature hub is occurring. As to be expected, the rotor of the IM is the hottest part. Due to the reduced convective heat transfer, the main heat dissipation is done by conductive heat transfer through the shaft, resulting in high temperatures of the front bearing and the shaft. The stator winding and the stator core are at low temperatures. During the following vehicle acceleration phase, the induction motor is turned off to allow the usage of the kinetic energy stored by the flywheel. As a result, the IM cools down. It can be observed, that the rotor components cool down slower than the stator components. This can be explained by the limited heat transfer due to the vacuum and the increased thermal capacitance due to the flywheel mounted on the same shaft. In general, higher temperatures can be observed in the low vehicle speed region of the WLTP driving cycle (in figure 7, from 3600 s to 4200 s). This is explained by the frequent still stand periods of the vehicle where the high speed IM is used to speed up the flywheel. In return, the kinetic energy is afterwards used to support the acceleration of the vehicle.

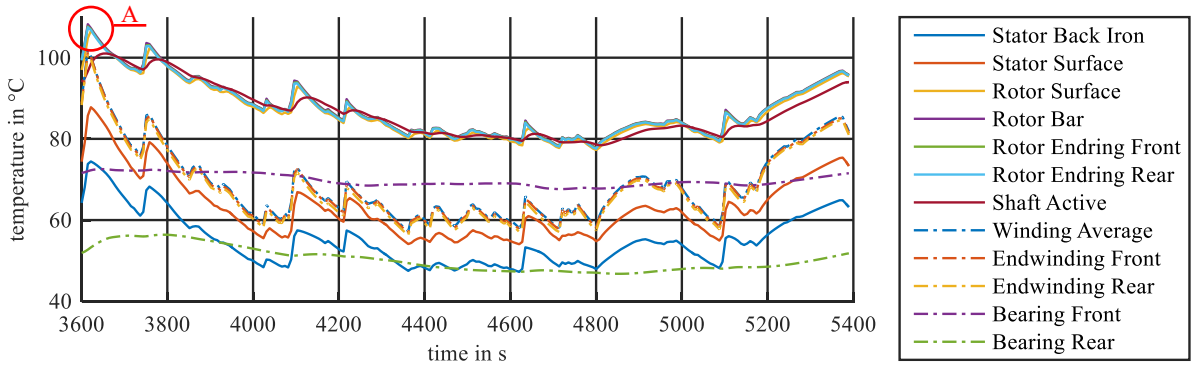

Fig. 7: Simulated temperature profile during a WLTP class 3 driving cycle.

During the medium vehicle speed region of the driving cycle (in figure 7, from 4200 s to 4600 s), the IM is used to keep the flywheel in its supposed speed region between 15,000 rpm and 45,000 rpm. Otherwise, the IM is not powered. As a result, the IM is cooled down. By a refinement of the operating strategy, the IM could be utilized for additional boost operations or smart energy management.

E. Structural FEA

To study the mechanical firmness of the high-speed rotor, mechanical stress simulations are performed. Linear-elastic material properties are used to speed up the simulation. However, for later validation of e.g. notch effects, phenomena like the supportive effect of ductile materials must be taken into consideration. To achieve realistic results, contact definitions and loads have to be well defined. Due to the temperature dependency of material properties, mainly the different thermal expansion of materials, and differing temperatures of parts in general, additional mechanical stress is applied to the assembly. Therefore, taking the temperatures into account is crucial to define realistic loads for the structural FEA [10]. From the results of the thermal simulation (Fig. 4), one critical operation point is identified at 3615 seconds with a motor speed of 45,000 rpm and temperatures of the parts according to Figure 4. This point of interest occurs after the initial speed up process of the flywheel. As simplification, the temperatures are evenly applied to the specific rotor component in the structural FEA carried out. For the prototypical build motor, a manufactured copper rotor is applied. The rotor bars are made of sectional rods. The short circuit rings are made of water jet cut copper discs which are laser welded onto the rotor bars. This allows the use of different materials for the rotor bars and the short circuit ring. In the current design, the rotor end rings are made of the copper alloy CuCrSiTi, which has a higher yield strength. Due to laser welding, bonded contacts between the rotor bars and the short circuit rings are assumed. Other than for the case of die-cast rotors, a relative movement between de rotor bars and the rotor slots can be expected in case of manufactured rotors. In the simulation, this is taken into account by a frictional contact. A small penetration of 5 µm takes the press fitting between the rotor bar and the slot into account. As a shaft-hub connection, a fit with an effective penetration of 26 µm is modeled. In addition, a lock nut is installed to further fasten the rotor stack. The lock nut provides a total axial force of 22.4 kN. To reduce the model size and therefore the computation time, symmetry of the rotor is utilized. Results of the simulation with linear elastic material properties are shown in Figure 5. Maximum von Mises stress occurs at the base of the rotor slots. The course of this mechanical stress can be considered as a notch effect. In reality, due to the supporting effect of ductile materials, in this case the electric steel, the stress peaks in this area are reduced as deeper zones take over a greater share of the mechanical stress.

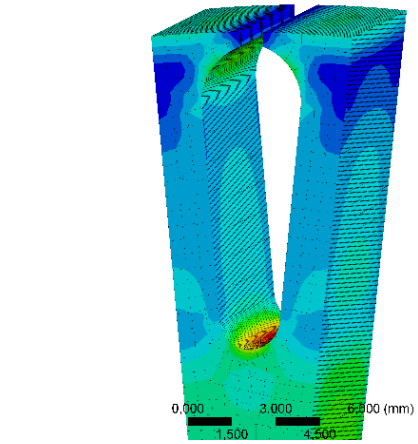

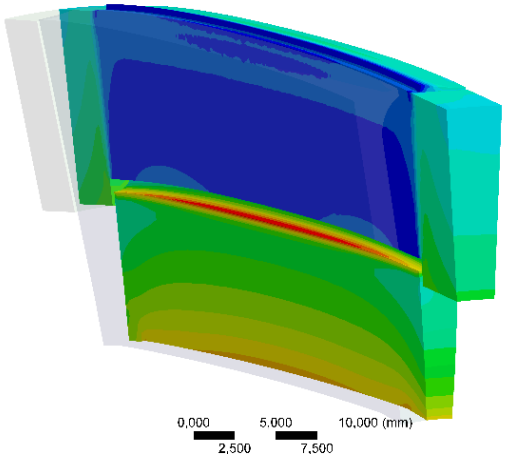

Fig. 8: Von-Mises stress in MPa at rotor slot (top) and at cut view along the stack including squirrel cage and rotor stack(bottom)

IV. Conclusions

In the work presented, a design methodology of a high-speed induction motor for a kinematic electric powertrain is developed. The design methodology followed consists of five steps which are described in this paper. Since an operating strategy of such a system for the applications mentioned does not exist, a combined development of the electric machine and the operating strategy is carried out. It is shown, that this approach allows for an efficient and highly utilized design. The methodology combines an accurate representation of the motor based on electromagnetic finite element analysis (FEA), a vehicle model including the powertrain and its operating strategy, transient thermal simulations of the motor and structural FEA of the high-speed rotor which gives the possibility of rapid refinement iterations in the fields of operating strategy, thermal circuit and mechanical firmness. The results of the transient thermal simulations show, that the utilization of the current design could be increased by a refinement of the operating strategy in use. Especially in medium vehicle speed regions, the IM could be used for additional boost operations or efficient energy management like providing additional electric energy in generator mode to reduce the load on the battery even more. The further refinement of the operating strategy is part of the future works. As a consequence, the results must be evaluated in regards of newly occurring critical operation conditions. The methodology described is used to review the impact on the systems performance, thermal aspects as well as the mechanical firmness of the motor.

Acknowledgment

This paper was developed in the context of the cooperative project ‘KinelectricDrive’, sponsored by the German Federal Ministry of Economic Affairs and Energy (BMWi), reference number 01MY14006B.

References

[1] S. Jurkovic, K. M. Rahman, and P. J. Savagian, “Design, optimization and development of electric machine for traction application in GM battery electric vehicle,” in *2015 IEEE International Electric Machines & Drives Conference (IEMDC)*: IEEE, 2015, pp. 1814–1819.

[2] T. Finken and K. Hameyer, “Design and optimization of an IPMSM with fixed outer dimensions for application in HEVs,” in *2009 IEEE International Electric Machines and Drives Conference*, 2009, pp. 1743–1748.

[3] J. Paulides, L. Encica, T. F. Beernaert, H. van der Velden, A. Parfant, and E. A. Lomonova, “Ultra-light-weight high torque density brushless PM machine design: Considering driving-cycle of a four-wheel drive race car,” in *2015 Tenth International Conference on Ecological Vehicles and Renewable Energies (EVER)*: IEEE, 2015, pp. 1–7.

[4] D. Butterweck, M. Hombitzer, D. Franck, and K. Hameyer, “KinelectricDrive - Hochdrehzahl Antriebssystem mit integriertem kinetischen Energiespeicher,” in *VDI-Berichte*, vol. 2268, *Antriebssysteme 2015: Elektrik, Mechanik, Fluidtechnik in der Anwendung ; Aachen, 11. und 12. November 2015*, Düsseldorf: VDI-Verl., 2015, pp. 3–13.

[5] H. A. Toliyat and G. B. Kliman, *Handbook of electric motors,* 2nd ed. New York: Marcel Dekker, 2004.

[6] A. L. Menn, W. R. Canders, and M. Henke, “Holistic analytical design of induction motors for automotive application,” in *2014 Ninth International Conference on Ecological Vehicles and Renewable Energies (EVER)*, 2014, pp. 1–7.

[7] G. von Pfingsten, A. Ruf, S. Steentjes, M. Hombitzer, D. Franck, and K. Hameyer, “Operating point resolved loss computation in electrical machines,” *Archives of Electrical Engineering*, vol. 65, no. 1, 2016.

[8] D. Staton, M. Popescu, C. Cossar, M. McGilp, S. Omori, and T. Kurimoto, “Analytical thermal models for small induction motors,” in *2008 18th International Conference on Electrical Machines*, 2008, pp. 1–6.

[9] P. W. Atkins and J. de Paula, *Physical chemistry,* 9th ed. New York: W.H. Freeman, 2010.

[10] T. Epskamp, B. Butz, and M. Doppelbauer, “Design and analysis of a high-speed induction machine as electric vehicle traction drive,” in *2016 18th European Conference on Power Electronics and Applications (EPE'16 ECCE Europe)*, 2016, pp. 1–10.